Chloride Ion Binding to Bacteriorhodopsin at Low pH: An Infrared Spectroscopic Study

4 AUTHORS, INCLUDING:

Lóránd Kelemen
Hungarian Academy of Sciences
60 PUBLICATIONS **576** CITATIONS

SEE PROFILE

Pal Ormos
Biological Research Centre, Hungarian Acad…
119 PUBLICATIONS **3,419** CITATIONS

SEE PROFILE

Chloride Ion Binding to Bacteriorhodopsin at Low pH: An Infrared Spectroscopic Study

Lóránd Kelemen, Péter Galajda, Sándor Száraz, and Pál Ormos
Institute of Biophysics, Biological Research Center of the Hungarian Academy of Sciences, Szeged, H-6701 Hungary

ABSTRACT   Bacteriorhodopsin (bR) and halorhodopsin (hR) are light-induced ion pumps in the cell membrane of *Halobacterium salinarium*. Under normal conditions bR is an outward proton transporter, whereas hR is an inward Cl^- transporter. There is strong evidence that at very low pH and in the presence of Cl^-, bR transports Cl^- ions into the cell, similarly to hR. The chloride pumping activity of bR is connected to the so-called acid purple state. To account for the observed effects in bR a tentative complex counterion was suggested for the protonated Schiff base of the retinal chromophore. It would consist of three charged residues: Asp-85, Asp-212, and Arg-82. This quadruplet (including the Schiff base) would also serve as a Cl^- binding site at low pH. We used Fourier transform infrared difference spectroscopy to study the structural changes during the transitions between the normal, acid blue, and acid purple states. Asp-85 and Asp-212 were shown to participate in the transitions. During the normal-to-acid blue transition, Asp-85 protonates. When the pH is further lowered in the presence of Cl^-, Cl^- binds and Asp-212 also protonates. The binding of Cl^- and the protonation of Asp-212 occur simultaneously, but take place only when Asp-85 is already protonated. It is suggested that HCl is taken up in undissociated form in exchange for a neutral water molecule.

INTRODUCTION

The plasma membrane of *Halobacterium salinarium* contains several retinal proteins. Two of them, bacteriorhodopsin (bR) and halorhodopsin (hR), serve as light-driven ion pumps. Both of them are intrinsic membrane proteins with largely similar structure: both are a complex of an all-*trans* retinal and an opsin with homologous sequence and structure. Their specific functions, however, are different. bR is a light-driven proton pump; upon light absorption it transports protons across the cell membrane outside the cell. On the other hand, hR pumps chloride ions (Cl^-) in the opposite direction, into the cell, upon light excitation. Questions of what are the important functional differences between these two proteins and what structural details cause the large differences in their functions have been intensively studied.

In hR two arginine residues are assumed to be Cl^- binding sites (Lányi et al., 1988; Oesterhelt and Tittor, 1989). Although bR also has two arginine residues in similar positions, their inability to bind Cl^- ions has been suggested to originate either in the low pK of these side chains or in some nearby negatively charged group hindering their Cl^- binding (Oesterhelt and Tittor, 1989).

It has been observed earlier that upon lowering the pH, bR undergoes characteristic changes. First, with a pK of about 2.5 its absorption shifts to 605 nm and the acid blue form (bR_{AB}) is formed (Oesterhelt and Stoeckenius, 1971; Mowery et al., 1979). If the pH is further lowered in the presence of Cl^- or other halide ions the original color is

regained and the acid purple state (bR_{AP}) is formed (Fischer and Oesterhelt, 1979). This form has been suggested to bind the Cl^- ion near the retinal binding site (Renthal et al., 1990).

Because, according to the logic of the comparison of the Cl^- binding ability of the arginine residues (Oesterhelt and Tittor, 1989) in bR and hR, the difference should vanish at low pH (by protonating either the low pK arginines or another nearby negative ion), Dér and co-workers raised the question whether bR_{AP} is capable of transporting Cl^-. Indeed, they have shown that when forming the acid purple form from the acid blue state, ion transport is regained (Dér et al., 1989). Although technical difficulties due to very low pH precluded explicit proof, all indirect tests were consistent with the assumption that the transported ion is Cl^-. Later, additional control experiments were performed, providing more circumstantial evidence (Keszthelyi et al., 1990; Dér et al., 1991).

When in bR, based on the analogous idea Asp-85 was exchanged for threonine with a much higher pK value, Cl^- transport could be directly demonstrated. It was already possible to measure this at normal pH values (Sasaki et al., 1995).

Although it has been questioned whether the acid purple form of bR exhibits any ion pumping activity (Moltke and Heyn, 1995), recent independent experiments reliably confirmed the original results (Kalaidzidis and Kaulen, 1997).

The paper by Dér et al. (1991) tentatively suggested a structure for the retinal binding site that could explain the basic differences between the normal, acid blue, and acid purple states. In this picture the counterion of the protonated Schiff base of the retinal binding site is a complex of three additional side chains, Asp-85, Asp-212, and Arg-82. This complex counterion would also provide the Cl^- binding site: in the normal and acid blue states a water molecule,

whereas in the acid purple state a Cl^- ion neutralizes the positive charge on the other side chains.

In this work we performed titration experiments to test the validity of this suggestion. We used Fourier Transform Infrared (FTIR) spectroscopy to determine changes between the normal, acid blue, and acid purple states of bR to characterize the retinal binding site in these three characteristic states.

MATERIALS AND METHODS

Instrumentation

Infrared spectra were recorded on a Bruker IFS 66S Fourier transform infrared spectrometer (Bruker Analytical Instruments, Karlsruhe, Germany) equipped with a standard DTGS detector and an external horizontal attenuated total reflection (ATR) sample holder (Spectratech, Stamford, CT). This accessory includes a 45° trapezoidal germanium crystal and is designed for liquids.

FT-Raman spectra were collected on the same spectrometer equipped with the FRA-106 Raman attachment (Bruker Analytical Instruments). Excitation in this instrument is achieved with a diode-pumped NdYAG laser (wavelength = 1066 nm).

A Shimadzu UV-160 spectrophotometer was used to measure the absorption spectra in the visible spectral region (Shimadzu Corporation, Kyoto, Japan).

Sample preparation

Purple membranes were isolated from *H. salinarium* strain S9 according to Oesterhelt and Stoeckenius (1974). The D85T protein was expressed in *H. salinarium* strain Pho81, which lacks all other bacterial opsins (Sasaki et al., 1995).

Sample preparation for the infrared measurements was the same as described in detail in Száraz et al. (1994). bR was first dried on the surface of the Ge crystal of the ATR cell and subsequently covered with the appropriate solution. Titration was achieved by exchanging the solution above the sample; because the sample was not touched during these procedures, the changes induced by modification of the bathing solution could be detected with very high sensitivity and accuracy. The solutions used to cover the bR film on top of the Ge crystal were combinations of HCl, NaCl, and H_2SO_4. The actual concentration of the particular components varied according to the desired pH or ion concentration. The pH of the solvent was always set by the appropriate HCl or H_2SO_4 concentration; no additional buffer was used. By using this method we avoided the disturbing effect of the infrared spectra of additional buffers. Because between 1000 and 1300 cm^{-1} there are very intense vibrations of the SO_4 group masking the fingerprint region, only the spectra above 1300 cm^{-1} could be evaluated. To rule out the possible effect of pH dependence on light adaptation, single beam spectra (250 double-sided, forward-backward scans, 2 cm^{-1} resolution) were taken at ambient light intensity where the sample was dark-adapted.

For the FT-Raman measurements purple membranes were embedded in 6% polyacrylamide gel (2 mm thick). This gel was attached to the front side of a 5-mm quartz cuvette that had a reflective coating on its back. The cuvette was then filled with the solution according to the particular titration experiment. When changing the bathing solution, the gel was removed from the cuvette and soaked in a large access volume of the new solution overnight to achieve complete and proper exchange.

We observed solvent effects in the infrared and Raman spectra. Therefore we also performed control measurements with the bathing solution and, only after appropriate scaling, subtracted this background to minimize the solvent bands.

Data processing

Infrared difference absorption spectra were calculated according to the equation $\Delta A_x = -\log_{10}(I_x/I_{ref})$, where I_{ref} and I_x are single beam spectra, I_{ref} is the selected reference spectrum, and x indicates pH or chloride concentration.

The difference spectra were fitted to a sum of Lorentzians. Because the titration experiments were expected to yield continuous changes in parameters common to all spectra, a global fit procedure was used. All spectra from a single titration experiment were fitted simultaneously, with the following coupling between the parameters: each curve was fit to the same number of Lorentzians, and the positions and widths of the corresponding Lorentzians were identical for each curve in the set. The amplitudes were allowed to be different from curve to curve. During the fit the common position and width values and the individual amplitude values were varied. The number of Lorentzians for the fit was determined by reasonable judgment: between 10 and 13 bands were necessary for a good description with sufficient detail in the regions discussed. In the protein bands certain fine structures (e.g., around 1500 cm^{-1} in Fig. 1 *b*) were ignored to prevent an escalation of the number of components. The fit procedure used the Levenberg-Marquardt least-squares minimization algorithm, performed with routines using the Matlab package (MathWorks, Inc., Natick, MA).

The resulting amplitudes of selected Lorentzians were used to determine pK_a values of the molecular transitions.

FIGURE 1   FTIR spectra measured during the acid titration of bR in the presence of 1M Cl^-. The solution contained 1M NaCl, the pH of the solution was set with 1 M HCl. The spectra reflect the difference induced by the pH change between the reference pH value and the pH value indicated in the curve. (*a*) Curves reflecting changes relative to pH = 7. (*b*) Curves reflecting changes relative to pH = 1.4. *Solid line*, measured data; *dashed line*, fit.

RESULTS

Our goal was to determine separately the effects of acidification and Cl^- binding. The procedure we applied to observe the two effects without permitting them to influence each other was based on the finding of Renthal et al. (1990) that acid and chloride effects can be separated using H_2SO_4. Two types of titration experiments were performed. First, acid titration was achieved at constant and saturating Cl^- concentration. Second, the effect of Cl^- was tested in a Cl^- titration experiment where proton concentration was kept at a saturating level: a constant pH of 0 was maintained while H_2SO_4 was exchanged for HCl. This approach was followed during the infrared, visible, and Raman measurements. During exchange of the solvent above the protein layer, in some cases, differences showed up due to changes in the sample thickness caused by the change of ionic composition or pH. These changes affected the amide regions and were not relevant in this study.

Investigation of the bR $\rightarrow$ bR_{AB} $\rightarrow$ bR_{AP} transition by acid titration in the presence of high Cl^- concentration

In the first series of measurements pH was lowered from 7 down to 0 by mixing appropriate amounts of 1 M HCl and 1 M NaCl (Fig. 1 a). According to Fischer and Oesterhelt (1979) and Váró and Lányi (1989), under these conditions both acidic states of bR form. Because the 1 M Cl^- concentration is high enough to saturate the Cl^- effect over the pH range where significant amount of bR_{AP} forms (Renthal et al., 1990), the transition is induced exclusively by the acidification of the bathing medium.

Fig. 1 a shows the series of infrared difference spectra obtained at different pH values. These spectra reflect changes in the structure relative to pH = 7. Although complete assignment of each band in this kind of spectra is not possible, we can make several firm assignments. For a review of the interpretation of infrared spectra of bR, see Rothschild (1992).

The protonated form of carboxylic acids has a characteristic frequency above 1680 cm^{-1} that originates from the $\nu_{C=O}$ bond stretch of the COOH group (Bellamy, 1980). In the bR difference spectra the region above 1700 cm^{-1} belongs exclusively to the COOH absorption; other vibrations can seldom reach such high frequencies. One possible source of ambiguity might be the $\nu_{C=O}$ mode of the ester group of lipids, but fortunately natural lipids in purple membrane do not have such esters (Stoeckenius et al., 1979). Consequently, we attribute the broad positive band above 1700 cm^{-1} (resolved to two Lorentzian bands centered at 1731 and 1713 cm^{-1}) to the protonation of several Asp or Glu side chains. The corresponding negative bands of disappearing COO^- are found at 1579 cm^{-1} and 1397 cm^{-1} (asymmetric and symmetric vibrations, respectively).

The change in the maxima of the visible absorption spectra due to the formation of the acidic forms is also reflected in the vibrational spectra as a shift of the frequency of the C $=$ C vibration of the retinal chromophore (Aton et al., 1977). Raman spectroscopy can be used as a tool to separate bands associated with chromophore vibrations from those of the protein. To separate the characteristic bands of the chromophore in the different states, we measured FT-Raman spectra under conditions identical to those of the infrared measurements (Fig. 2). Results agree well with the resonance Raman spectra of Smith and Mathies (1985), although there are slight differences in peak positions and relative amplitudes, probably due to the near-infrared excitation used in our case (Sawatzki et al., 1990; Rath et al., 1993). According to the Raman data, we assigned the complex features of the infrared difference spectra depicted in Fig. 1 in the region of $\sim$1510–1530 cm^{-1} to the ethylenic vibrations of the chromophore. In accordance with the literature (Smith and Mathies, 1985; de Groot et al., 1990), our Raman data indicate that chromophore bands not only shift during these transitions but also differ because of the altered retinal isomeric composition in the different acidic states. The Raman spectrum (Fig. 2) of bR clearly shows two overlapping bands, indicating that a mixture of 13-*cis* and all-*trans* retinal is present (full width at the half maximum (FWHM) is 22 cm^{-1}). In the bR_{AB} spectra only one band can be seen but, according to the relatively high 23 cm^{-1} FWHM of the band, it is reasonable to suppose this form to exist in dark-adapted form, too. In the bR_{AP} states only one band can be seen and its FWHM suggests that in this state, the sample is only in all-*trans* form. Due to this complexity, curve fitting to Lorentzians was not able to completely resolve the spectral changes in the ethylenic region of the infrared spectra in Fig. 1 a but performed very well under conditions where only the transition between bR_{AB} and bR_{AP} was observed (Fig. 1 b and Fig. 5).

The acidic forms of bR were originally identified by their visible absorption spectra (Fig. 3 a) therefore to support the
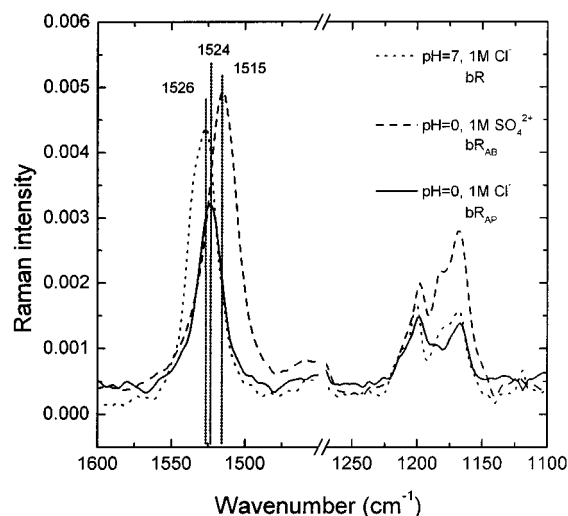

FIGURE 2 FT-Raman spectra measured in the bR, bR_{AB}, and bR_{AP} states. The actual H^+ and Cl^- concentrations were set by using 1 M HCl, 1 M H_2SO_4 and 1 M NaCl.
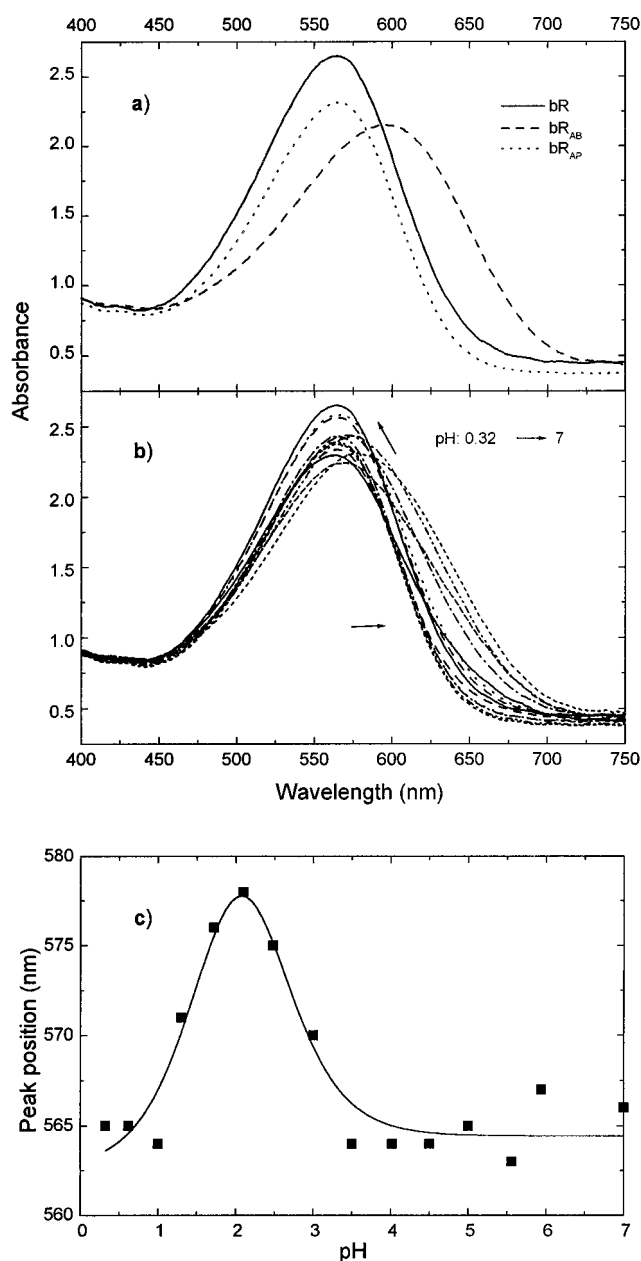
FIGURE 3 Visible spectroscopy of the acid titration of bR in the presence of 1M Cl$^-$. (*a*) The spectra of the characteristic states of bR (bR, bR$_{AB}$, and bR$_{AP}$). (*b*) The evolution of the spectra with changing pH. (*c*) The position of the absorption maxima as a function of pH. The solid line represents a fit to two pK values: pK$_1$ = 2.3 and pK$_2$ = 1.33.

infrared data we performed analogous experiments in the visible spectral region, too (Fig. 3 *b*). Under these conditions the data could be evaluated by assuming two pK$_a$ values (Fig. 3 *c*). A global curve fitting to all amplitudes with Eq. 1 resulted in pK$_{a1}$ = 2.3 and pK$_{a2}$ = 1.33 for the bR → bR$_{AB}$ and bR$_{AB}$ → bR$_{AP}$ transitions, respectively.

To derive pK$_a$ values from the infrared data the difference spectra were first deconvoluted to a sum of Lorentzians by the global fit procedure (see Materials and Methods). The pH dependence of the amplitudes of the Lorentzians were

then used to calculate the pK$_a$ values (pK$_{a1}$ = 2.97 and pK$_{a2}$ = 1.39). For the bR$_{AB}$ → bR$_{AP}$ transition there is a good agreement between the titration experiments performed in the visible and in the infrared. However, for the bR → bR$_{AB}$ transition, the titration followed in the infrared yields a significantly higher pK$_a$ value. A reasonable explanation is given below for the difference.

On the spectra shown in Fig. 1 *a* it is apparent that the bands characteristic to carboxylic groups change considerably in the pH region between 3 and 1.4. It was shown previously that during the formation of bR$_{AB}$ about 14 water-exposed carboxyl groups become protonated (Gerwert et al., 1987). Based on the pK$_a$ values of carboxylic side chains of amino acids in solutions (pK$_a$ = 3.9 for aspartic acid and pK$_a$ = 4.3 for glutamic acid), the protonation of these groups would be expected to take place in a pH region higher than the range of our measurements. Moreover, based on the large relative size, broadness, and inhomogeneity of the bands in the 1750–1700 cm^{-1} spectral range and around 1390 cm^{-1}, we assigned these spectral changes to these water-accessible carboxylic groups of bR. According to our data about two-thirds of these surface groups get protonated only when pH < 3, coinciding with the pH range where the bR$_{AB}$ transition occurs. In ^{13}C cross-correlation magic angle spinning (CP-MAS) NMR experiments Metz et al. (1992) found correlation between the color change during the bR → bR$_{AB}$ transition and the protonation state of Asp-85: the purple-to-blue transition occurs parallel with the protonation of the negatively charged Asp-85 in the complex counterion of the Schiff base. Because this crucial protonation coincides with the protonation of several other carboxylic groups of the molecule, we were unable to separate the expected spectral changes that were unambiguously due to the proton uptake of only Asp-85; they were also not seen by Gerwert et al. (1987). This argument also explains why the pK value for the bR → bR$_{AB}$ transitions obtained from the FTIR spectra is considerably higher than that obtained from the visible spectra. In the titration followed in the infrared the protonation of surface carboxylic groups with pK close to the bulk may also contribute, thus apparently shifting the pK of the transition to a higher value.

To reveal spectral changes attributed to the formation of bR$_{AB}$ we have calculated difference spectra using the single beam spectrum measured at pH = 1.4 as the reference (Fig. 1 *b*). Because this value is close to the midpoint of the bR$_{AB}$ → bR$_{AP}$ transition, negative bands in these spectra are characteristic of those of bR$_{AB}$, whereas the positive ones are characteristic of those of bR$_{AP}$. This is confirmed by the appearance of a negative band at 1511 cm^{-1} that can be attributed to the ethylenic stretch of the bR$_{AB}$ chromophore and a positive band at 1524 cm^{-1} due to bR$_{AP}$. In the FT-Raman spectra we have found the values of 1516 cm^{-1} and 1526 cm^{-1}, respectively (Fig. 2). In the region of the $\nu_{C=O}$ vibration of COOH groups we have found two bands, a negative one at 1754 cm^{-1} and a positive one at 1727 cm^{-1}. Note that the amplitude of the 1727 cm^{-1} band is

about twice that of the one seen at 1754 cm^{-1}. The appearance of a 1387-cm^{-1} negative band characteristic of a carboxylate anion indicates that an Asp or Glu residue having its carbonyl frequency at 1727 cm^{-1} became protonated during the transition. It is very unreasonable to suppose that a carboxyl group would deprotonate upon increasing proton concentration; consequently, we attribute the 1754 cm^{-1} negative band to the effect of Cl^{-} binding induced by the lowered pH.

Investigation of the bR$_{AB}$ → bR$_{AP}$ transition by Cl^{-} titration

In the second set of experiments proton concentration was kept at a constant value of ≈1 M (pH = 0) high enough to saturate proton binding. In this series of experiments, first pH = 0 was set by 1 M H$_2$SO$_4$ and this was gradually exchanged to 1 M HCl to increase Cl^{-} concentration. At the beginning of the experiment (in 1 M H$_2$SO$_4$) the pigment is in the bR$_{AB}$ state but in 1 M HCl complete transition to the bR$_{AP}$ state is reached (Renthal et al., 1990). As the proton concentration was kept constant in these experiments, the bR$_{AB}$ → bR$_{AP}$ transition was induced by Cl^{-} binding.

The result of these experiments is shown in Fig. 4. The ethylenic bands are similar to the ones in the spectra depicted in Fig. 1 b and clearly show that conversion from bR$_{AB}$ (as indicated by the negative band at 1511 cm^{-1}) to bR$_{AP}$ (as indicated by the positive band at 1521 cm^{-1}) occurs during the experiment. It is interesting to look at the bands characteristic of carboxylic groups. In the region of

the carbonyl stretching vibrations of COOH groups we have obtained the same changes as in the acid titration: a negative band at 1752 cm^{-1} and a positive one at 1729 cm^{-1}. Here also, the 1729 cm^{-1} band has an amplitude twice that of the band at 1752 cm^{-1}. The negative band at 1389 cm^{-1} associated with the carboxylate anion is also present. This confirms that all of these spectral features are characteristic of the bR$_{AB}$ → bR$_{AP}$ transition and are not dependent on whether the transition was induced by acidification in the presence of Cl^{-} ions or by adding Cl^{-} ions at pH = 0.

To provide experimental data to further explore the origin of the carboxylic bands, we performed control experiments on the D85T mutant of bR. The structure of the complex counterion in this mutant is similar to hR and it was shown to bind and pump Cl^{-} ions even under physiological conditions (Sasaki et al., 1995). Fig. 6 shows the change of the infrared spectrum upon Cl^{-} binding at pH = 0.

DISCUSSION

Assignment of spectral changes to individual groups of bR

The spectral changes in the region of the carboxylic vibrations show essentially the same features independent of whether the transition was induced by acidification in the presence of high Cl^{-} concentration or by addition of Cl^{-} ions at high proton concentration (Figs. 1 and 4). Similar spectral changes were also obtained in comparable experiments of other groups. Marrero and Rothschild (1987) investigated the structural changes associated with the formation of bR$_{AB}$ in an experiment similar to ours. Because they used HCl to change pH, not only bR$_{AB}$ but also bR$_{AP}$ has been formed in their experiment. By using only HCl to set the pH, it is not possible to separate the effects of Cl^{-} binding and H^{+} binding. Although their paper does not

FIGURE 4   FTIR measurement of the Cl^{-} titration experiment. The pH of the solution was kept constant at pH = 0, while H$_2$SO$_4$ was exchanged to HCl. The spectra reflect the differences due to the exchange of SO$_4^{2-}$ to Cl^{-} referenced to the state with only SO$_4^{2-}$ to the Cl^{-} concentration marked above the curves. *Solid line*, measured data; *dashed line*, fit.
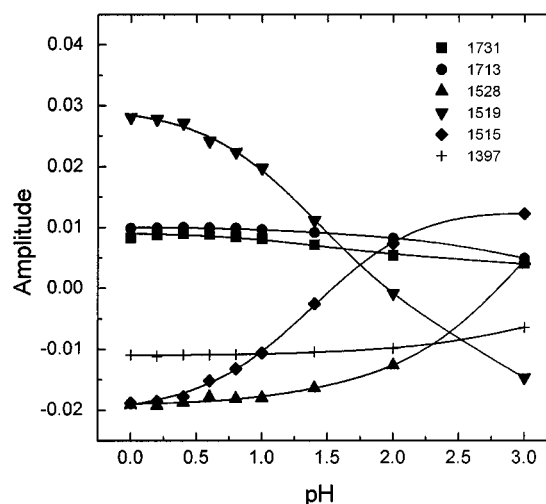

FIGURE 5   The change of the amplitudes of selected Lorentzians fitted to the infrared spectra during the acid titration experiment. The curves are the result of the global fit with two pK values, pK$_1$ = 2.97 and pK$_2$ = 1.33.
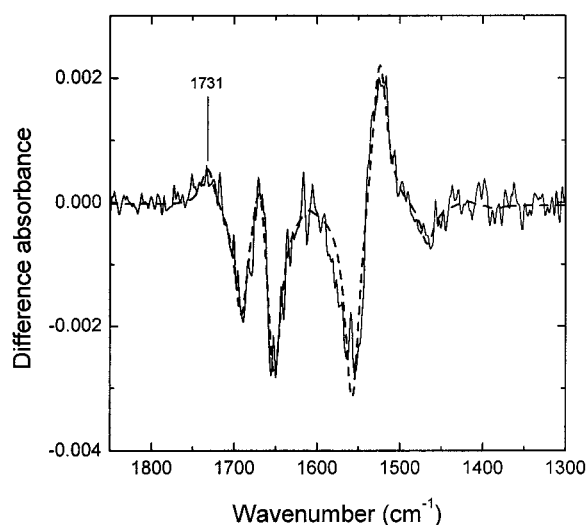
FIGURE 6 Difference spectra of bR mutant D85T between 0 and 1 M Cl^- at pH = 0. *Solid line*, measured data; *dashed line*, fit.

explicitly discuss it, if one compares the ethylenic and COOH bands with our data, the presence of bR_{AP} is apparent at low pH, e.g., in the pH = 1.8 to pH = 1.4 difference spectra, a negative ethylenic band demonstrates the loss of bR_{AB} (1509 cm^{-1}) and a positive one the formation of bR_{AP} (1524 cm^{-1}). In agreement with our data, there is a negative band at 1755 cm^{-1} and a positive one at 1732 cm^{-1}. The $bR_{AB} \rightarrow bR_{AP}$ transition was investigated by Le Coutre et al. (1995). In this investigation, the conversion to bR_{AP} was induced by blowing HCl gas onto a pellet of purple membranes originally in the acid blue state. The obtained peak positions were 1515 cm^{-1} and 1531 cm^{-1} for the ethylenic bands and 1762 and 1731 cm^{-1} for the negative and positive carboxylic bands, respectively. These features were essentially unchanged in the Arg-82 mutant. Based on the well known light-induced M-bR difference spectra (M is a photocycle intermediate), the negative band at 1762 cm^{-1} was attributed to Asp-85 and it was assumed to downshift to 1733 cm^{-1} upon Cl^- binding. A similarly high frequency, 1754 cm^{-1}, was suggested for Asp-85 by Masuda et al. (1995) from the study of deionized blue bR. Mitrovich et al. (1995) assigned the peak at 1732 cm^{-1} to Asp-85 in the bR_{AP} state by investigating the bR_{AP} photocycle on wild-type bR and mutants. Although the paper does not state this, its figures suggest that Asp-212 is protonated also in the bR_{AP} state and its frequency is around 1730 cm^{-1}. In contrast, Braiman et al. (1996) provided experimental evidence that the COOH band of Asp-85 in unphotolyzed bR is found at 1723 cm^{-1}. This conclusion was obtained from an experiment similar to ours, but the infrared difference spectrum was calculated only between two nearby pH values, close to the pK_a of the bR $\rightarrow$ bR_{AB} transition. Our data covering a much broader pH range clearly show that in the pH region where the formation of bR_{AB} from bR is observed, the COOH bands change much more than would be expected from the protonation of only one COOH band. We

suggest that the big size and unusual broadness of the cited band is due to the protonation of a number of water-exposed carboxyl groups that protonate with a pK_a significantly lower than a typical aspartate or glutamate pK_a (≈ 4) in solution. A similar conclusion was drawn by Marrero and Rothschild (1987), who found that upon acidification of purple membranes most of the carboxyl protonation changes occur in the pH range between 3 and 2. As we have seen earlier, the higher pK_a value obtained from the fit to the data from the FTIR experiment for the bR $\rightarrow$ bR_{AB} transition also points to the fact that protonation of carboxyl groups not directly connected to the color change takes place in this pH region, which is higher than the actual transition but lower than the bulk value. Therefore, we believe that the broad 1723 cm^{-1} band belongs to these water-accessible groups.

The above arguments also explain why we could not separately observe the protonation of Asp-85 during the bR $\rightarrow$ bR_{AB} transition (Fig. 1). The large and inhomogeneous band that extends from 1690 cm^{-1} to 1760 cm^{-1} due to the several other water-accessible acidic groups masks the Asp-85 band as it extends over the frequency region where the COOH group of Asp-85 is also expected to appear. NMR data indicated a rather hydrophobic environment for Asp-85 both in the M state of the photocycle and in the ground state bR (Metz et al., 1992). The carbonyl frequency of a carboxyl group depends on the polarizability of the environment (Bellamy, 1980; Dioumaev and Braiman, 1995). This would favor assignment of the higher frequencies to Asp-85 close to the value observed in the M form.

The control experiments performed on the bR mutant D85T helped to identify the side chains with the carboxylic groups responsible for the observed changes during the binding of Cl^- (Fig. 6). Although due to the instability of the mutant sample under the measuring conditions the quality of this spectrum is not as good as in the case of wild-type bR, it is evident that the positive carboxyl band is preserved around 1730 cm^{-1} but the negative one at the higher frequency is missing. Assuming that Cl^- is bound by a similar mechanism to this mutant as it is to wild-type bR, the most obvious source of the band at 1731 cm^{-1} is Asp-212. Due to the instability of the mutant sample the Cl^- titration caused more expressed amide changes that can be followed clearly in the amide I and II regions. These amide bands are large enough to mask the shift in the C = C region that reflects the color change of the sample.

In conclusion, taking into account the arguments above and our results on the D85T mutant of bR, we attribute the negative carboxyl band at 1754 cm^{-1} (Fig. 1 *b*) and 1752 cm^{-1} (Fig. 4) to Asp-85 and the positive band at 1727 cm^{-1} (Fig. 1 *b*) and at 1729 cm^{-1} (Fig. 4) to Asp-212 and Asp-85. Using this identification, one can relate the observed spectral changes to the following molecular events. Based on the NMR experiments of de Groot et al. (1990), we attribute the positive carboxyl band found at 1730 cm^{-1} to the protonation of Asp-212. To explain that upon formation of bR_{AP} the

localization of the electric charges around the Schiff base is practically identical to that of bR, as it was concluded from the comparison of their visible absorption and Raman spectra (Smith and Mathies, 1985) and study of bR mutants (Marti et al., 1991), to substitute its negative charge in the bR_{AP} state the bound Cl^- ion must reside close to Asp-85. The appearance of the Cl^- anion close to the retinal binding site (highly apolar in the bR_{AB} state) induces changes in the region that probably include the appearance of one or more water molecules, or may involve H bonding to the COOH carbonyl. The increase of polarizability (dielectric constant) as well as H bonding result in a downshift of the carbonyl frequency (Dioumaev and Braiman, 1995) to approximately 1730 cm^{-1}, according to our data. This frequency shift explains the negative band at around 1750 cm^{-1} and the fact that the amplitude of the 1730 cm^{-1} band is about twice as large as the negative band at 1750 cm^{-1} (similar to the spectra of Le Coutre et al., 1995), i.e., at 1730 cm^{-1} the COOH vibration of both Asp-85 and Asp-212 in the bR_{AP} state is seen. The presence of the negative band at 1390 cm^{-1} (the loss of COO^-) confirms that protonation of a carboxylic group occurs upon formation of bR_{AP} and spectral changes cannot be explained only by the shift of the carbonyl band of a single protonated carboxyl group. It is also very improbable that anion binding itself would change the intensity of the carbonyl band to such an extent. Because, according to our data, Cl^- binding is negligible until most of bR is converted into bR_{AB} and significantly increases below the pK_a of this transition (the apparent dissociation constant is 1.5 M at pH = 2 but it goes down to 35 mM at pH = 0, according to Renthal et al. (1990)), we conclude that one of the prerequisites of halide anion binding is the protonation of Asp-85. It is more interesting to discuss the role of Asp-212. NMR measurements showed that only Asp-85 gets protonated in the absence of halide anions upon acidification; protonation of Asp-212 was observed exclusively in the bR_{AP} form (de Groot et al., 1990; Metz et al., 1992). Our data also show that acidification in the presence of Cl^- induces the protonation of Asp-212 along with the binding of the anion to the complex counterion as indicated by the ethylenic bands, but interestingly, protonation of Asp-212 also occurs if the pH is kept constant and sulfate anions are exchanged for Cl^-. This suggests that protonation of Asp-212 occurs in parallel with Cl^- binding, but only if Asp-85 is already protonated. Protonation of Asp-212 and Cl^- binding can apparently take place only simultaneously. We suggest therefore that Cl^- is picked up in the form of undissociated HCl (and an H_2O molecule is released in exchange) and dissociates inside the protein. The feasibility of such a reaction was shown in a molecular dynamics simulation of HCl ionization at the surface of stratospheric ice (Gertner and Hynes, 1996).

All of these findings confirm with independent experiments the validity of the model for the structure of the Schiff base counterion in the different acidic states introduced in Dér et al. (1991). NMR data (de Groot et al., 1990)

support the theory that in the $bR_{AB} \rightarrow bR_{AP}$ transition, Cl^- is exchanged for an OH^- or H_2O is exchanged for dissociated HCl.

In the case of hR two anion binding sites were suggested (Lányi, 1990) and both were hypothetically assigned to positively charged arginine residues. In fact, it was shown that in the hR mutant R108Q the chloride transport was completely inactivated. In bR_{AP} the role of Arg-82 in Cl^- binding is not yet clear. The band that would indicate the perturbation of the guanidino group of Arg-82 by the bound Cl^- is expected between 1650 cm^{-1} and 1690 cm^{-1} (Braiman et al., 1994). The negative peak at 1690 cm^{-1} in Fig. 6 has an amplitude comparable to the amide change, so this is too large in both amplitude and width to be a reasonable candidate to represent the change of a single Arg peak. Unfortunately, in our case we have the poorest signal-to-noise ratio in the 1600–1700 cm^{-1} region due to the high water absorption in this region. In addition, the assignment of small bands is unreliable because of the overlap with the amide I band; consequently a reliable statement about the Arg side chain cannot be made. Le Coutre and co-workers (1995) found only very small influence of the replacement of Arg-82 by a lysine on the $bR_{AB} \rightarrow bR_{AP}$ transition and suggested that Arg-82 does not play a specific role in anion binding. Thus, although the groups Asp-85 and Asp-212 have clearly been shown to participate directly in the complex counterion and Cl^- binding, the necessary additional positive group has still to be identified.

REFERENCES

Aton, B., A. G. Doukas, R. H. Callender, B. Becher, and T. G. Ebrey. 1977. Resonance Raman studies of the purple membrane. *Biochemistry.* 16: 2995–2998.

Bellamy, L. J. 1980. The Infrared Spectra of Complex Molecules. Chapman and Hall, London.

Braiman, M. S., A. K. Dioumaev, and J. R. Lewis. 1996. A large photolysis-induced pK_a increase of the chromophore counterion in bacteriorhodopsin: implications for ion transport mechanisms of retinal proteins. *Biophys. J.* 70:939–947.

Braiman, M. S., T. J. Walter, and D. Briercheck. 1994. Infrared spectroscopic detection of light-induced change in chloride-arginine interaction in halorhodopsin. *Biochemistry.* 33:1629–1635.

Le Coutre, J., M. Rüdiger, D. Oesterhelt, and K. Gerwert. 1995. FTIR investigation of the blue to acid-purple transition of Bacteriorhodopsin by use of induced halide binding. *J. Mol. Struct.* 349:165–168. de Groot, H. J. M., S. O. Smith, J. Courtin, E. van den Berg, C. Winkel, J. Lugtenburg, R. G. Griffin, and J. Herzfeld. 1990. Solid-state ^{13}C and ^{15}N NMR study of the low pH forms of bacteriorhodopsin. *Biochemistry.* 29:6873–6883.

Dér, A., R. Tóth-Boconádi, and L. Keszthelyi. 1989. Bacteriorhodopsin as a possible chloride pump. *FEBS Lett.* 259:24–26.

Dér, A., S. Száraz, R. Tóth-Boconádi, Zs. Tokaji, L. Keszthelyi, and W. Stoeckenius. 1991. Alternative translocation of protons and halide ions by bacteriorhodopsin. *Proc. Natl. Acad. Sci. USA.* 88:4751–4755.

Dioumaev, A. K., and M. S. Braiman. 1995. Modelling vibrational spectra of amino acid side chains in proteins: the carbonyl stretch frequency of buried carboxylic residues. *J. Am. Chem. Soc.* 117:10572–10574.

Fischer, U., and D. Oesterhelt. 1979. Chromophore equilibria in bacteriorhodopsin. *Biophys. J.* 28:211–230.

Gertner, B. J., and J. Hynes. 1996. Molecular dynamics simulation of hydrochloric ionization at the surface of stratospheric ice. *Science.* 271:1563–1566.

Gerwert, K., U. M. Ganter, F. Siebert, and B. Hess. 1987. Only water exposed carboxyl-groups are protonated during the transition to the cation-free blue bacteriorhodopsin. *FEBS Lett.* 213:39–44.

Kalaidzidis, I. V., and A. D. Kaulen. 1997. Cl^- dependent photovoltage responses of bacteriorhodopsin: comparison of the D85T and D85S mutants and wild-type acid purple form. *FEBS Lett.* 418:239–242.

Keszthelyi, L., S. Száraz, A. Dér, and W. Stoeckenius. 1990. Bacteriorhodopsin and halorhodopsin: multiple ion pumps. *Biochim. Biophys. Acta.* 1018:260–262.

Lányi, J. K. 1990. Halorhodopsin: a light-driven electrogenic chloride transport system. *Physiol. Rev.* 70:319–330.

Lányi, J. K., L. Zimányi, K. Nakanishi, F. Derguini, M. Okabe, and B. Honig. 1988. Chromophore/protein and chromophore/anion interactions in halorhodopsin. *Biophys. J.* 53:185–191.

Marrero, H., and K. J. Rothschild. 1987. Bacteriorhodopsin's M_{412} and BR_{605} protein conformations are similar. *FEBS Lett.* 223:289–293.

Marti, T., S. J. Rösselet, H. Otto, M. P. Heyn, and H. G. Khorana. 1991. The retinylidene Schiff-base counterion in bacteriorhodopsin. *J. Biol. Chem.* 288:18674–18683.

Masuda, S., M. Nara, M. Tasumi, M. A. El-Sayed, and J. K. Lányi. 1995. Fourier transform infrared studies of the effect of Ca^{2+} binding on the states of aspartic acid side chains in bacteriorhodopsin. *J. Phys. Chem.* 99:7776–7781.

Metz, G., F. Siebert, and M. Engelhardt. 1992. Asp-85 is the only internal aspartic acid that gets protonated in the M intermediate and the purple-to-blue transition of bacteriorhodopsin. *FEBS Lett.* 303:237–241.

Mitrovich, Q. M., G. V. Kenneth, and M. S. Braiman. 1995. Differences between the photocycles of halorhodopsin and the acid purple form of bacteriorhodopsin analyzed with millisecond time-resolved FTIR spectroscopy. *Biophys. Chem.* 56:121–127.

Moltke, S., and M. P. Heyn. 1995. Photovoltage kinetics of the acid-blue and acid-purple forms of bacteriorhodopsin: evidence for no net charge transfer. *Biophys. J.* 69: 2066–2073.

Mowery, P. C., R. H. Lozier, Q. Chae, Y. W. Tseng, M. Taylor, and W. Stoeckenius. 1979. Effect of acid pH on the absorption spectra and photoreactions of bacteriorhodopsin. *Biochemistry.* 18:4100–4107.

Oesterhelt, D., and W. Stoeckenius. 1971. Rhodopsin-like protein from the purple membrane of *Halobacterium halobium. Nature New Biol.* 233:149–152.

Oesterhelt, D., and W. Stoeckenius. 1974. Isolation of the cell membrane of *Halobacterium halobium* and its fractionation into red and purple membrane. *Methods Enzymol.* 31:667–668.

Oesterhelt, D., and J. Tittor. 1989. Two pumps, one principle: light-driven ion transport in halobacteria. *Trends Biol. Sci.* 14:57–61.

Rath, P., M. P. Krebs, Y. He, H. G. Khorana, and K. J. Rothschild. 1993. Fourier transform Raman spectroscopy of the bacteriorhodopsin mutant Tyr-185→Phe: formation of a stable O-like species during light adaptation and detection of its transient N-like photoproduct. *Biochemistry.* 32:2272–2281.

Renthal, R., K. Shuler and R. Regalado. 1990. Control of bacteriorhodopsin color by chloride at low pH: significance for the proton pump mechanism. *Biochim. Biophys. Acta.* 1016:378–384.

Rothschild, K. J. 1992. FTIR difference spectroscopy of bacteriorhodopsin: toward a molecular model. *J. Bioenerg. Biomemb.* 24:147–167.

Sasaki, J., L. S. Brown, Y.-S. Chon, H. Kandori, A. Maeda, R. Needleman, and J. K. Lányi. 1995. Conversion of bacteriorhodopsin into a chloride ion pump. *Science.* 269:73–75.

Sawatzki, J., R. Fischer, H. Scheer, and F. Siebert. 1990. Fourier-transform Raman spectroscopy applied to photobiological systems. *Proc. Natl. Acad. Sci. USA.* 87:5903–5906.

Smith, O. S., and R. A. Mathies. 1985. Resonance Raman spectra of the acidified and deionized forms of bacteriorhodopsin. *Biophys. J.* 47:251–254.

Stoeckenius, W., R. H. Lozier, and R. A. Bogomolni. 1979. Bacteriorhodopsin and the purple membrane of halobacteria. *Biochim. Biophys. Acta.* 505:215–27.

Száraz, S., D. Oesterhelt, and P. Ormos. 1994. pH-induced structural changes in bacteriorhodopsin studied by Fourier transform infrared spectroscopy. *Biophys. J.* 67:1706–1712.

Váró, G., and J. K. Lányi. 1989. Photoreactions of bacteriorhodopsin at acid pH. *Biophys. J.* 56:1143–1151.